Acta Cryst E CRYSTALLOGRAPHIC COMMUNICATIONS

ISSN 2056-9890

Crystal structure and Hirshfeld surface analysis, crystal voids, interaction energy calculations and energy frameworks of *C*-anthracen-9-yl-*N*-methyl aldonitrone

Jamal Lasri,[a]* Mohamed M. Zayed,[a,b] Yaseen A. Almehmadi,[a,c] Naser E. Eltayeb,[a,d] Tuncer Hökelek[e] and Aidan P. McKay[f]

[a]Department of Chemistry, Rabigh College of Science and Arts, King Abdulaziz University, Jeddah 21589, Saudi Arabia, [b]Environmental and Occupational Medicine Department, National Research Centre, Giza 12622, Egypt, [c]King Fahd Medical Research Center, King Abdulaziz University, Jeddah 21589, Saudi Arabia, [d]Department of Chemistry, Faculty of Pure and Applied Sciences, International University of Africa, Khartoum 2469, Sudan, [e]Department of Physics, Hacettepe University, 06800 Beytepe, Ankara, Türkiye, and [f]EaStCHEM School of Chemistry, University of St Andrews, Fife KY16 9ST, United Kingdom. *Correspondence e-mail: jlasri@kau.edu.sa

Received 6 January 2026
Accepted 21 January 2026

Edited by L. Van Meervelt, Katholieke Universiteit Leuven, Belgium

Keywords: *C*-anthracen-9-yl-*N*-methyl aldonitrone; crystal structure; hydrogen bond; π-stacking; Hirshfeld surface; energy framework analysis.

CCDC reference: 2524759

Supporting information: this article has supporting information at journals.iucr.org/e

The title compound (systematic name: 1-anthracen-9-yl-*N*-methylmethanimine oxide), $C_{16}H_{13}NO$, contains an almost planar anthracene ring system [r.m.s. deviation = 0.021 (1) Å]. In the crystal, intermolecular bifurcated C—H···O hydrogen bonds link the molecules into infinite chains along the *a*-axis direction. The π–π stacking interactions between the benzene rings of adjacent molecules help to consolidate the three-dimensional architecture. The Hirshfeld surface analysis of the crystal structure indicates that the most important contributions for the crystal packing are from H···H (54.5%), H···C/C···H (23.7%), H···O/O···H (10.6%) and C···C (9.8%) interactions. The volume of the crystal voids and the percentage of free space were calculated to be 76.07 Å^3 and 6.57%, respectively, showing that there is no large cavity in the crystal packing. Evaluation of the electrostatic, dispersion and total energy frameworks indicates that the stabilization largely depends on dispersion energy contributions. Hydrogen bonding, π–π and van der Waals interactions, together with the dispersion energy contributions, are the dominant interactions in the crystal packing.

1. Chemical context

Nitrones have interesting applications as buiding blocks in the synthesis of natural products (Padwa & Pearson, 2002) and have found usage as both modifiers in radical polymerization and regulators of molecular weight (Feuer, 2007; Hamer & Macaluso, 1964). Nitrones have been broadly used in metal-mediated [2 + 3]-cycloaddition reactions to furnish N-heterocyclic compounds which have shown to be excellent catalysts for Suzuki-Miyaura C—C cross-couplings (Fernandes *et al.*, 2011). Nitrones have also been used for therapeutic applications as they are components of the molecular structure of several drugs (Floyd *et al.*, 2008). Currently, our research program focuses on the synthesis, X-ray structure analysis, Hirshfeld surface analysis and density functional theory (DFT) calculations and molecular docking studies of aldonitrone-type compounds (Lasri *et al.*, 2024). Herein, we report the synthesis, molecular and crystal structures, Hirshfeld surface analysis, crystal voids, interaction energies and energy frameworks of the title compound *C*-anthracen-9-yl-*N*-methyl aldonitrone, (I).

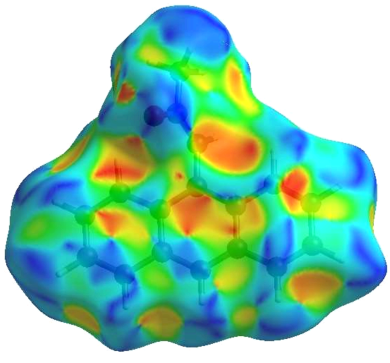

OPEN ACCESS
Published under a CC BY 4.0 licence

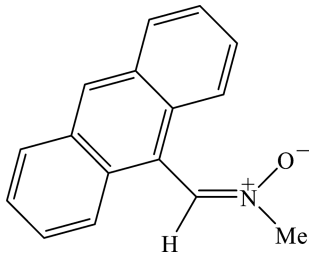

2. Structural commentary

The title compound, (I), contains an almost planar [r.m.s. deviation = 0.021 (1) Å] anthracene ring system, consisting of three fused benzene rings, denoted *A* (C1/C2/C7–C9/C14), *B* (C2–C7) and *C* (C9–C14) (Fig. 1). Atom C3 deviates by −0.0419 (14) Å from the least-squares plane through the ring system. The planes of benzene rings *A*, *B* and *C* are oriented at dihedral angles of *A*/*B* = 1.95 (4)°, *A*/*C* = 1.99 (5)° and *B*/*C* = 0.51 (3)°. In the substituent, the C1—C15—N16, C15—N16—C17, C15—N16—O16 and C17—N16—O16 bond angles are 125.01 (13), 119.73 (12), 125.30 (12) and 114.96 (11)°, respectively. On the other hand, the N16—C15—C1—C2, N16—C15—C1—C14, C15—C1—C2—C3 and C15—C1—C14—C13 torsion angles are 56.39 (19), −128.50 (14), −1.4 (2) and 4.96 (19)°, respectively. The dihedral angle between the plane of the anthracene ring and the least-squares plane through its substituent is 54.42 (5)°.

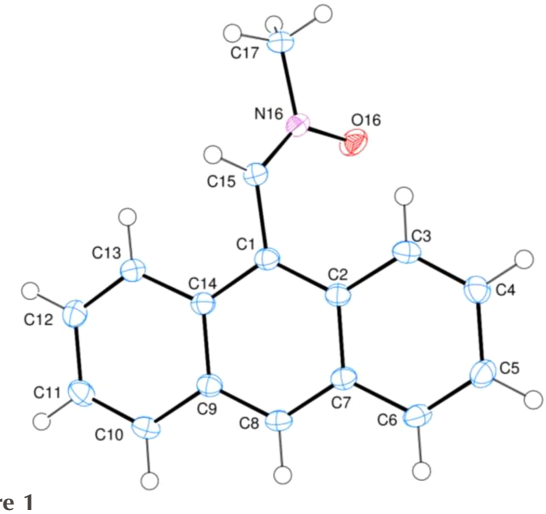

Figure 1
The molecular structure of the title molecule with the atom-numbering scheme and 50% probability displacement ellipsoids.

3. Supramolecular features

In the crystal, intermolecular bifurcated C—H···O hydrogen bonds (Table 1) link the molecules into infinite chains along the *a*-axis direction (Fig. 2). The *π*–*π* stacking interactions between the benzene rings (*A*, *B* and *C*) of adjacent molecules, with inter-centroid distances of 3.8445 (8) [between rings *A* and *B*, *α* = 1.96 (6)° and slippage = 1.592 Å] and 3.8497 (8) Å [between rings *A* and *C*, *α* = 0.51 (7)° and slippage = 1.636 Å] may help to consolidate the three-dimensional architecture, together with C—H···O contacts. No C—H···*π*(ring) interactions are identified.

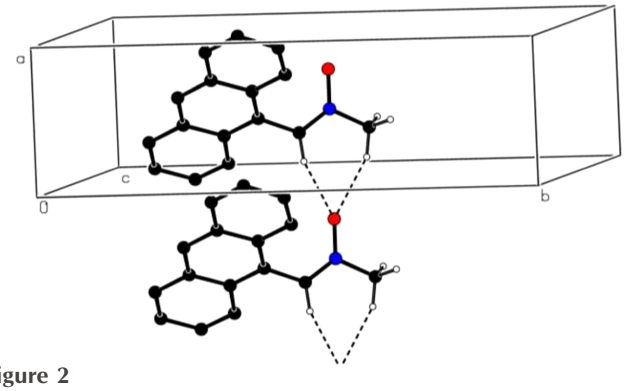

Figure 2
A partial packing diagram viewed down the *c*-axis direction. Intermolecular C—H···O hydrogen bonds are shown as dashed lines. Nonbonding H atoms have been omitted for clarity.

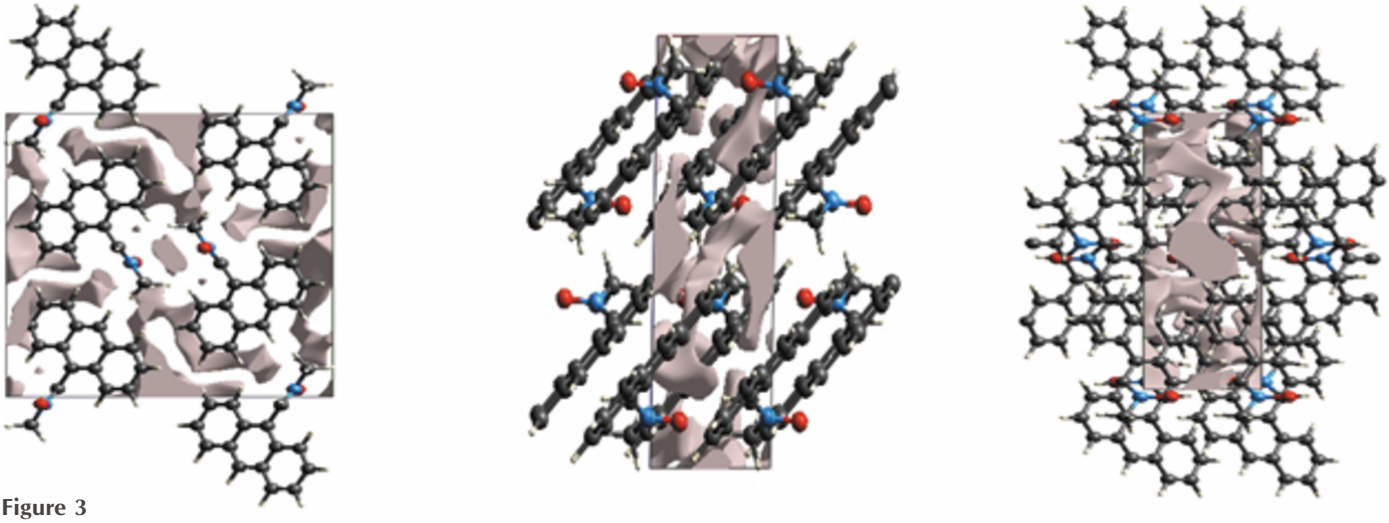

Figure 3
Graphical views of voids in the crystal packing of the title compound (*a*) along the *a*-axis, (*b*) along the *b*-axis and (*c*) along the *c*-axis direction.

Table 1
Hydrogen-bond geometry (Å, °).

D—H···A	D—H	H···A	D···A	D—H···A
C15—H15···O16^{i}	0.95	2.24	3.1267 (18)	154
C17—H17B···O16^{i}	0.98	2.28	3.2037 (18)	157

Symmetry code: (i) $x+1, y, z$.

A void analysis was performed by adding up the electron densities of the spherically symmetric atoms contained in the asymmetric unit (Turner *et al.*, 2011). The volume of the crystal voids [Figs. 3(*a*), 3(*b*) and 3(*c*)] and the percentage of free space in the unit cell are calculated as 76.07 Å^3 and 6.57%, respectively, indicating that the crystal packing is compact.

4. Hirshfeld surface analysis

A Hirshfeld surface (HS) analysis was carried out using *CrystalExplorer* (Version 17.5; Spackman *et al.*, 2021) for clarifying the intermolecular interactions in the crystal of (I). The HS plotted over $d_{\rm norm}$ is shown in Fig. 4, where the bright-red spots correspond to donor and/or acceptor sites; they also appear as blue and red regions in Fig. 5, corresponding to positive and negative potentials (Spackman *et al.*, 2008). The shape-index surface can be used for identifying the characteristic packing modes, particularly, the presence of aromatic stacking interactions like C—H···π(ring) and π–π interactions, with the former represented as red π-holes, which are related to the electron–ring interactions between the C—H groups with the centroids of the aromatic rings of neighbouring molecules. Fig. 6 clearly suggests that there are no C—H···π(ring) interactions. A π–π stacking is indicated by the presence of adjacent red and blue triangles, as clearly indicated by Fig. 6. According to the 2D fingerprint plots (McKinnon *et al.*, 2007), intermolecular H···H, H···C/C···H, H···O/O···H and C···C contacts make important contributions to the HS, with values of 54.5, 23.7, 10.6 and 9.8%, respectively (Fig. 7).

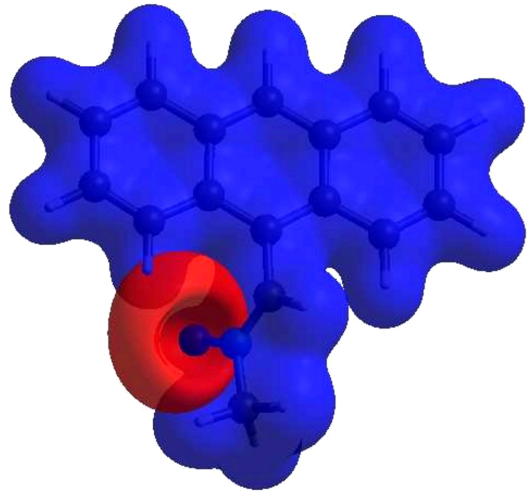

Figure 5
View of the Hirshfeld surface of the title compound plotted over electrostatic potential energy in the range from −0.0500 to 0.0500 a.u. using the STO-3G basis set at the Hartree–Fock level of theory. Hydrogen-bond donors and acceptors are shown as blue and red regions around the atoms corresponding to positive and negative potentials, respectively.

5. Database survey

A survey of the Cambridge Structural Database (CSD, Version 6.01, November 2025 update; Groom *et al.*, 2016) revealed 3581 C9-substituted anthracene derivatives. Herein, we present 20 of them with structural similarity to the target compound *C*-anthracen-9-yl-*N*-methyl aldonitrone, namely, **I** (AWUZOI; Kraicheva *et al.*, 2011), **II** (AXODAS; Wong *et al.*, 2004), **III** (AZORUD; Geetha *et al.*, 2011), **IV** (CEJLOT; Horiguchi & Ito, 2006), **V** (CUBMOC; Jaworska *et al.*, 2009), **VI** (EDOHIS; Monika *et al.*, 2022), **VII** (FAXVIK; Howie *et al.*, 2005), **VIII** (FIBQIT; Spinelli *et al.*, 2018), **IX** (FOHLOE; Howie & Wardell, 2005), **X** (GUMLAD; Lohar *et al.*, 2015), **XI** (KEYJAD; Kakimoto *et al.*, 2023), **XII** (KOBWAC; Ghosh *et al.*, 2017), **XIII** (NIJWEK; Banerjee *et al.*, 2013), **XIV** (NOKMIN; Zheng *et al.*, 2024), **XV** (OCOLUQ; Faizi *et al.*,

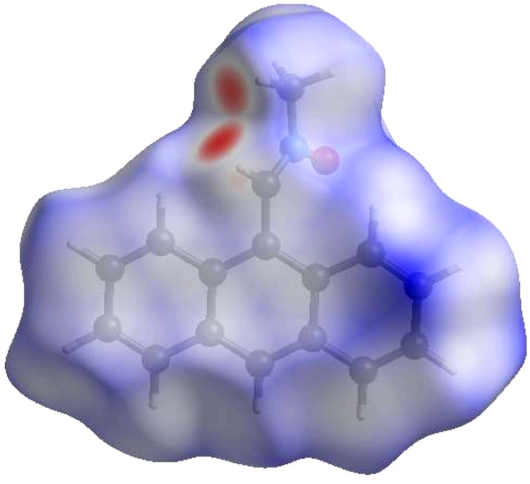

Figure 4
View of the three-dimensional Hirshfeld surface of the title compound plotted over $d_{\rm norm}$ in the range from −0.3681 to 1.4279 a.u.

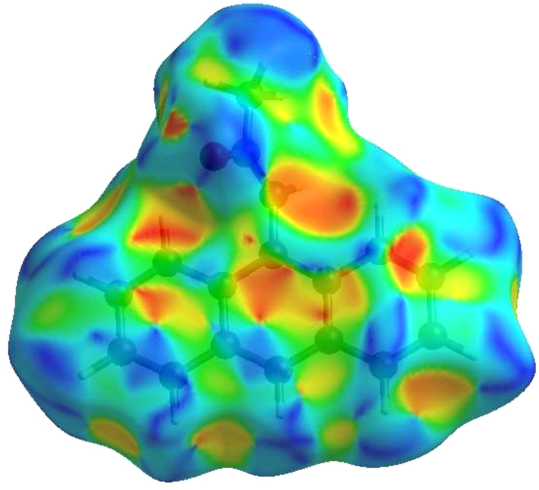

Figure 6
Hirshfeld surface of the title compound plotted over shape-index.

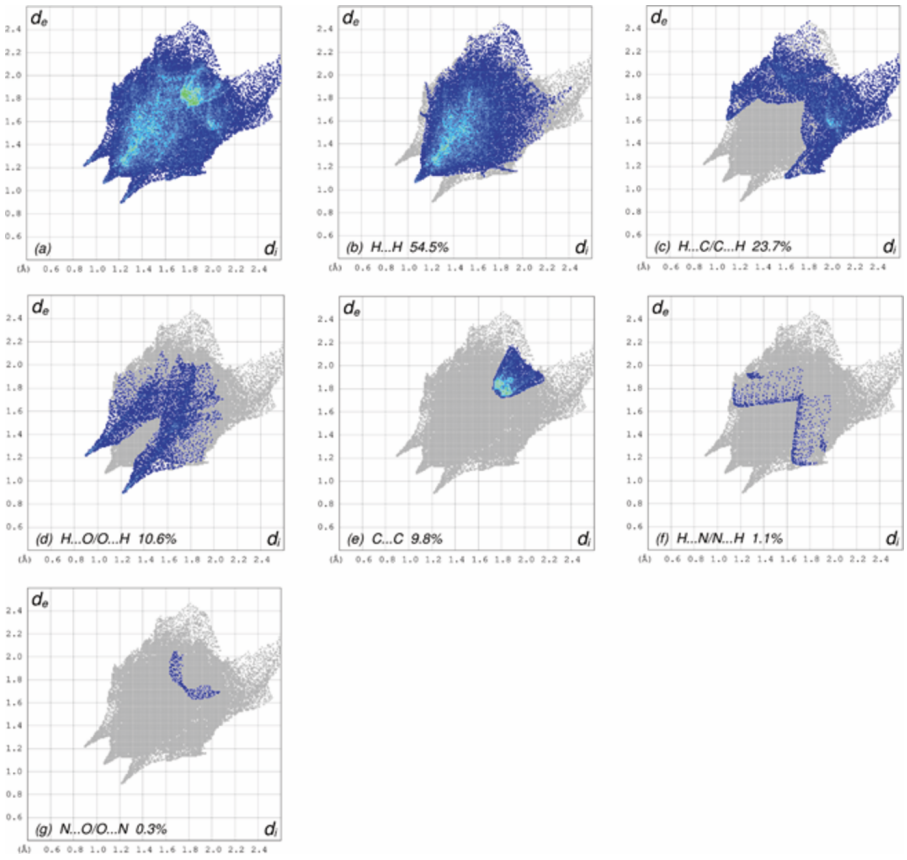

Figure 7
The full two-dimensional fingerprint plots for the title compound, showing (*a*) all interactions, and delineated into (*b*) H···H, (*c*) H···C/C···H, (*d*) H···O/O···H, (*e*) C···C, (*f*) H···N/N···H and (*g*) N···O/O···N interactions. The d_i and d_e values are the closest internal and external distances (in Å) from given points on the Hirshfeld surface contacts.

2017), **XVI** (PIGWOR; Subramanian *et al.*, 1993), **XVII** (QARBUG; Ihmels *et al.*, 2000), **XVIII** (TITNES; Junor *et al.*, 2019), **XIX** (TUPGIV; Villalpando *et al.*, 2010) and **XX** (YIVQAY; Barwiolek *et al.*, 2019).

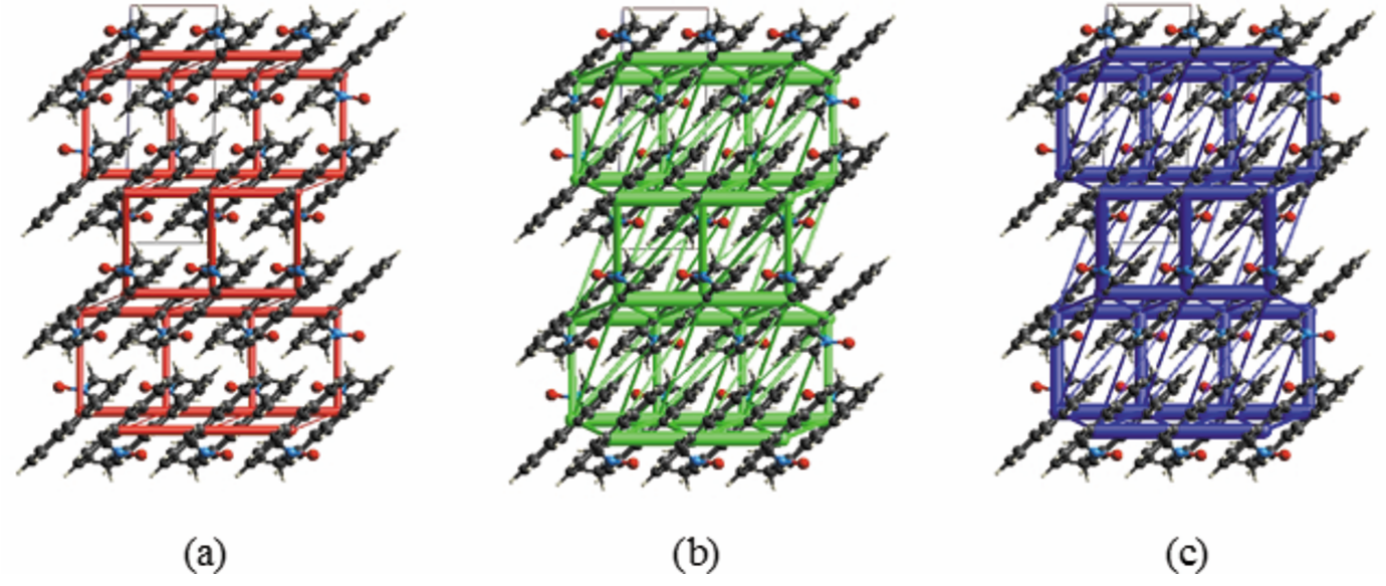

Figure 8
The energy frameworks for a cluster of molecules of the title compound viewed down the *b* axis, showing the (*a*) electrostatic energy E_{ele}, (*b*) dispersion energy E_{dis} and (*c*) total energy E_{tot} diagrams. The cylindrical radius is proportional to the relative strength of the corresponding energies and they were adjusted to the same scale factor of 80 with a cut-off value of 5 kJ mol^{-1} within 2×2×2 unit cells.

Table 2
Experimental details.

Crystal data	
Chemical formula	$C_{16}H_{13}NO$
M_r	235.27
Crystal system, space group	Monoclinic, $P2_1/n$
Temperature (K)	100
a, b, c (Å)	4.89615 (14), 16.6590 (5), 14.2008 (4)
β (°)	91.240 (3)
V (Å^3)	1158.02 (6)
Z	4
Radiation type	Mo $K\alpha$
μ (mm^{-1})	0.08
Crystal size (mm)	0.26 × 0.02 × 0.01
Data collection	
Diffractometer	Rigaku XtaLAB P200K
Absorption correction	Multi-scan (*CrysAlis PRO*; Rigaku OD, 2024)
T_{min}, T_{max}	0.714, 1.000
No. of measured, independent and observed [$I > 2\sigma(I)$] reflections	24788, 2788, 1992
R_{int}	0.055
(sin $\theta/\lambda)_{max}$ (Å^{-1})	0.682
Refinement	
$R[F^2 > 2\sigma(F^2)]$, $wR(F^2)$, S	0.043, 0.124, 1.05
No. of reflections	2788
No. of parameters	164
H-atom treatment	H-atom parameters constrained
$\Delta\rho_{max}$, $\Delta\rho_{min}$ (e Å^{-3})	0.30, −0.20

Computer programs: *CrysAlis PRO* (Rigaku OD, 2024), *SHELXT2018* (Sheldrick, 2015*a*), *SHELXL2019* (Sheldrick, 2015*b*) and *OLEX2* (Dolomanov *et al.*, 2009).

6. Interaction energy calculations and energy frameworks

The CE-B3LYP/6-31G(d,p) energy model available in *CrystalExplorer* (Version 17.5; Spackman *et al.*, 2021) was used to calculate the intermolecular interaction energies. Hydrogen-bonding interaction energies (in kJ mol^{-1}) were calculated to be −33.9 (E_{ele}), −10.9 (E_{pol}), −62.7 (E_{dis}), 65.8 (E_{rep}) and −57.9 (E_{tot}) for the C15—H15···O16, and −23.9 (E_{ele}), −6.4 (E_{pol}), −32.8 (E_{dis}), 18.5 (E_{rep}) and −47.1 (E_{tot}) for the C17—H17*B*···O16 hydrogen-bond interaction. Energy frameworks combine the calculation of intermolecular interaction energies with a graphical representation of their magnitude (Turner *et al.*, 2015). Energy frameworks were constructed for E_{ele} (red cylinders), E_{dis} (green cylinders) and E_{tot} (blue cylinders) [Figs. 8(*a*), 8(*b*) and 8(*c*)], and their evaluation indicates that the stabilization largely depends on dispersion energy contributions in the crystal structure of (I).

7. Synthesis and crystallization

To a solution of *N*-methylhydroxylamine (99.9 mg, 1.20 mmol) in MeOH (50 ml) was added sodium carbonate (63.4 mg, 0.60 mmol) and the reaction mixture was stirred for 10 min followed by the addition of anthracene-9-carbaldehyde (224.4 mg, 1.09 mmol). The mixture was then stirred for 12 h at room temperature. The precipitate which formed was filtered off and MeOH was eliminated *in vacuo*. In order to remove the NaCl produced, the obtained solid was dissolved in CH_2Cl_2 and filtered, the filtrate was then evaporated *in vacuo*. The solid product was ultimately washed with Et_2O to give pure *C*-anthracen-9-yl-*N*-methyl aldonitrone, (I). Yellow crystals suitable for X-ray analysis were obtained by slow evaporation of a CH_2Cl_2 solution (yield 90%). FT–IR (cm^{-1}): 1637 (C═N), 1566 (C═C). Analysis calculated (%) for $C_{16}H_{13}NO$: C 81.68, H 5.57, N 5.95; found: C 81.73, H 5.60, N 5.93.

8. Refinement

Crystal data, data collection and structure refinement details are summarized in Table 2. The C-bound H-atom positions were calculated geometrically at distances of 0.95 (for aromatic and methine CH) and 0.98 Å (for CH_3), and refined using a riding model by applying the constraints $U_{iso}(H) = kU_{eq}(C)$, where k = 1.5 for CH_3 and 1.2 for the other H atoms.

Acknowledgements

The authors would like to thank D. B. Cordes for his fruitful discussion. TH is grateful to Hacettepe University Scientific Research Project Unit.

Funding information

Funding for this research was provided by: Hacettepe Üniversitesi (grant No. 013 D04 602 004).

References

Banerjee, A., Sahana, A., Das, A., Lohar, S., Sarkar, B., Mukhopadhyay, S. K., Sanmartín Matalobos, J. & Das, D. (2013). *Dalton Trans.* **42**, 16387–16395.

Barwiolek, M., Wojtczak, A., Kozakiewicz, A., Babinska, M., Tafelska-Kaczmarek, A., Larsen, E. & Szlyk, E. (2019). *J. Lumin.* **211**, 88–95.

Dolomanov, O. V., Bourhis, L. J., Gildea, R. J., Howard, J. A. K. & Puschmann, H. (2009). *J. Appl. Cryst.* **42**, 339–341.

Faizi, M. S. H., Haque, A., Ahmad, M. & Golenya, I. A. (2017). *Acta Cryst.* E**73**, 137–140.

Fernandes, R. R., Lasri, J., da Silva, M. F. C. G., Palavra, A. M. F., da Silva, J. A. L., da Silva, J. J. R. F. & Pombeiro, A. J. L. (2011). *Adv. Synth. Catal.* **353**, 1153–1160.

Feuer, H. (2007). *Nitrile oxides, nitrones, and nitronates*, in *Organic synthesis: novel strategies in synthesis*, 2nd ed. New Jersey: John Wiley & Sons Inc.

Floyd, R. A., Kopke, R. D., Choi, C.-H., Foster, S. B., Doblas, S. & Towner, R. A. (2008). *Free Radic. Biol. Med.* **45**, 1361–1374.

Geetha, K., Kumar, D. K. A. P., Lakshmanan, D., Savitha, R. & Murugavel, S. (2011). *Acta Cryst.* E**67**, o2577.

Ghosh, M., Ghosh, A., Ta, S., Matalobos, J. S. & Das, D. (2017). *Chem. Sel.* **2**, 7426–7431.

Groom, C. R., Bruno, I. J., Lightfoot, M. P. & Ward, S. C. (2016). *Acta Cryst.* B**72**, 171–179.

Hamer, J. & Macaluso, A. (1964). *Chem. Rev.* **64**, 473–495.

Horiguchi, M. & Ito, Y. (2006). *J. Org. Chem.* **71**, 3608–3611.

Howie, R. A., Kindness, A., McKay, M. G. & Maguire, G. E. M. (2005). *Acta Cryst.* E**61**, o52–o54.

Howie, R. A. & Wardell, S. M. S. V. (2005). *Acta Cryst.* E**61**, o1686–o1688.

Ihmels, H., Leusser, D., Pfeiffer, M. & Stalke, D. (2000). *Tetrahedron* **56**, 6867–6875.
Jaworska, M., Łączkowski, K. Z., Wełniak, M., Welke, M. & Wojtczak, A. (2009). *Appl. Catal. Gen.* **357**, 150–158.
Junor, G. P., Romero, E. A., Chen, X., Jazzar, R. & Bertrand, G. (2019). *Angew. Chem. Int. Ed.* **58**, 2875–2878.
Kakimoto, Y., Ikemura, R., Imai, Y., Tohnai, N., Yamazaki, S., Nakata, E. & Takashima, H. (2023). *RSC Adv.* **13**, 1914–1922.
Kraicheva, I., Tsacheva, I., Vodenicharova, E., Tashev, E. & Troev, K. (2011). *Acta Cryst.* E**67**, o1980.
Lasri, J., Soliman, S. M., Ali, E. M. M., Eltayeb, N. E., Dege, N., Donia, T., Khamis, A. A. & Alzahrani, F. A. (2024). *J. Mol. Struct.* **1312**, 138624.
Lohar, S., Safin, D. A., Sengupta, A., Chattopadhyay, A., Matalobos, J. S., Babashkina, M. G., Robeyns, K., Mitoraj, M. P., Kubisiak, P., Garcia, Y. & Das, D. (2015). *Chem. Commun.* **51**, 8536–8539.
McKinnon, J. J., Jayatilaka, D. & Spackman, M. A. (2007). *Chem. Commun.* pp. 3814–3816.
Monika, Verma, A., Tiwari, M. K., Subba, N. & Saha, S. (2022). *J. Photochem. Photobiol. A: Chem.* **433**, 14130.
Padwa, A. & Pearson, W. H. (2002). In *Synthetic application of 1,3-dipolar cycloaddition chemistry toward heterocycles and natural products*. New Jersey: John Wiley & Sons Inc.
Rigaku OD (2024). *CrysAlis PRO*. Rigaku Corporation, Tokyo, Japan
Sheldrick, G. M. (2015*a*). *Acta Cryst.* A**71**, 3–8.
Sheldrick, G. M. (2015*b*). *Acta Cryst.* C**71**, 3–8.
Spackman, M. A., McKinnon, J. J. & Jayatilaka, D. (2008). *CrystEngComm* **10**, 377–388.
Spackman, P. R., Turner, M. J., McKinnon, J. J., Wolff, S. K., Grimwood, D. J., Jayatilaka, D. & Spackman, M. A. (2021). *J. Appl. Cryst.* **54**, 1006–1011.
Spinelli, F., d'Agostino, S., Taddei, P., Jones, C. D., Steed, J. W. & Grepioni, F. (2018). *Dalton Trans.* **47**, 5725–5733.
Subramanian, R., Koch, S. A. & Harbison, G. S. (1993). *J. Phys. Chem.* **97**, 8625–8629.
Turner, M. J., McKinnon, J. J., Jayatilaka, D. & Spackman, M. A. (2011). *CrystEngComm* **13**, 1804–1813.
Turner, M. J., Thomas, S. P., Shi, M. W., Jayatilaka, D. & Spackman, M. A. (2015). *Chem. Commun.* **51**, 3735–3738.
Villalpando, A., Fronczek, F. R. & Isovitsch, R. (2010). *Acta Cryst.* E**66**, o1353.
Wong, W. Y., Lu, G. L., Liu, L., Shi, J. X. & Lin, Z. (2004). *Eur. J. Inorg. Chem.* pp. 2066–2077.
Zheng, Y., Chen, P., Niu, Z. & Wang, E. (2024). *Spectrochim. Acta A Mol. Biomol. Spectrosc.* **312**, 124035.

supporting information

Acta Cryst. (2026). E**82**, 221-226 [https://doi.org/10.1107/S2056989026000599]

Crystal structure and Hirshfeld surface analysis, crystal voids, interaction energy calculations and energy frameworks of *C*-anthracen-9-yl-*N*-methyl aldonitrone

Jamal Lasri, Mohamed M. Zayed, Yaseen A. Almehmadi, Naser E. Eltayeb, Tuncer Hökelek and Aidan P. McKay

Computing details

1-Anthracen-9-yl-*N*-methylmethanimine oxide

Crystal data

$C_{16}H_{13}NO$
M_r = 235.27
Monoclinic, $P2_1/n$
a = 4.89615 (14) Å
b = 16.6590 (5) Å
c = 14.2008 (4) Å
β = 91.240 (3)°
V = 1158.02 (6) Å^3
Z = 4
$F(000)$ = 496
D_x = 1.349 Mg m^{-3}
Mo $K\alpha$ radiation, λ = 0.71073 Å
Cell parameters from 8143 reflections
θ = 2.8–29.1°
μ = 0.08 mm^{-1}
T = 100 K
Platy-needle, yellow
0.26 × 0.02 × 0.01 mm

Data collection

Rigaku XtaLAB P200K diffractometer
Radiation source: Rotating Anode, Rigaku FR-X
Rigaku Osmic Confocal Optical System monochromator
Detector resolution: 5.8140 pixels mm^{-1}
shutterless scans
Absorption correction: multi-scan (CrysAlis PRO; Rigaku OD, 2024)
T_{min} = 0.714, T_{max} = 1.000
24788 measured reflections
2788 independent reflections
1992 reflections with $I > 2\sigma(I)$
R_{int} = 0.055
θ_{max} = 29.0°, θ_{min} = 1.9°
h = −6→6
k = −21→21
l = −19→19

Refinement

Refinement on F^2
Least-squares matrix: full
$R[F^2 > 2\sigma(F^2)]$ = 0.043
$wR(F^2)$ = 0.124
S = 1.05
2788 reflections
164 parameters
0 restraints
Primary atom site location: dual
Hydrogen site location: inferred from neighbouring sites
H-atom parameters constrained
$w = 1/[\sigma^2(F_o^2) + (0.0587P)^2 + 0.3266P]$ where $P = (F_o^2 + 2F_c^2)/3$
$(\Delta/\sigma)_{max}$ < 0.001
$\Delta\rho_{max}$ = 0.30 e Å^{-3}
$\Delta\rho_{min}$ = −0.20 e Å^{-3}

Special details

Geometry. All esds (except the esd in the dihedral angle between two l.s. planes) are estimated using the full covariance matrix. The cell esds are taken into account individually in the estimation of esds in distances, angles and torsion angles; correlations between esds in cell parameters are only used when they are defined by crystal symmetry. An approximate (isotropic) treatment of cell esds is used for estimating esds involving l.s. planes.

Fractional atomic coordinates and isotropic or equivalent isotropic displacement parameters (Å²)

	x	*y*	*z*	U_{iso}*/U_{eq}
O16	0.2639 (2)	0.47437 (6)	0.60736 (7)	0.0281 (3)
N16	0.5270 (2)	0.47324 (7)	0.61726 (8)	0.0205 (3)
C1	0.5642 (3)	0.60243 (8)	0.70066 (9)	0.0178 (3)
C2	0.3685 (3)	0.60047 (8)	0.77210 (9)	0.0175 (3)
C3	0.2557 (3)	0.52728 (8)	0.80734 (9)	0.0204 (3)
H3	0.315933	0.477410	0.782852	0.025*
C4	0.0635 (3)	0.52796 (8)	0.87536 (9)	0.0229 (3)
H4	−0.009682	0.478649	0.897013	0.028*
C5	−0.0289 (3)	0.60146 (9)	0.91436 (9)	0.0232 (3)
H5	−0.166736	0.601175	0.960406	0.028*
C6	0.0801 (3)	0.67197 (8)	0.88573 (9)	0.0215 (3)
H6	0.021220	0.720677	0.913543	0.026*
C7	0.2818 (3)	0.67444 (8)	0.81452 (9)	0.0183 (3)
C8	0.3977 (3)	0.74681 (8)	0.78584 (9)	0.0192 (3)
H8	0.341342	0.795398	0.814553	0.023*
C9	0.5936 (3)	0.74962 (8)	0.71628 (9)	0.0186 (3)
C10	0.7105 (3)	0.82395 (8)	0.68640 (10)	0.0222 (3)
H10	0.655215	0.872636	0.715162	0.027*
C11	0.8991 (3)	0.82603 (8)	0.61756 (10)	0.0244 (3)
H11	0.973665	0.875937	0.598406	0.029*
C12	0.9852 (3)	0.75359 (9)	0.57416 (10)	0.0243 (3)
H12	1.118288	0.755476	0.526533	0.029*
C13	0.8788 (3)	0.68159 (8)	0.60015 (9)	0.0211 (3)
H13	0.937397	0.633996	0.569781	0.025*
C14	0.6800 (3)	0.67635 (8)	0.67244 (9)	0.0178 (3)
C15	0.6736 (3)	0.52877 (8)	0.65776 (9)	0.0196 (3)
H15	0.866041	0.521447	0.659962	0.024*
C17	0.6620 (3)	0.40225 (8)	0.57657 (10)	0.0228 (3)
H17A	0.608897	0.354042	0.611222	0.034*
H17B	0.860711	0.408976	0.581280	0.034*
H17C	0.606005	0.396676	0.510219	0.034*

Atomic displacement parameters (Å²)

	U^{11}	U^{22}	U^{33}	U^{12}	U^{13}	U^{23}
O16	0.0163 (6)	0.0333 (6)	0.0348 (6)	0.0009 (4)	0.0017 (4)	−0.0111 (5)
N16	0.0171 (6)	0.0207 (6)	0.0237 (6)	0.0009 (5)	0.0036 (5)	−0.0040 (5)
C1	0.0172 (7)	0.0170 (7)	0.0191 (6)	0.0021 (5)	−0.0013 (5)	−0.0019 (5)
C2	0.0184 (7)	0.0162 (6)	0.0178 (6)	0.0020 (5)	−0.0011 (5)	−0.0002 (5)

C3	0.0243 (8)	0.0153 (6)	0.0216 (7)	0.0028 (5)	−0.0002 (6)	−0.0013 (5)
C4	0.0286 (8)	0.0201 (7)	0.0202 (7)	−0.0024 (6)	0.0030 (6)	0.0020 (5)
C5	0.0246 (8)	0.0259 (7)	0.0194 (6)	0.0013 (6)	0.0055 (6)	0.0008 (6)
C6	0.0245 (8)	0.0194 (7)	0.0208 (6)	0.0052 (6)	0.0032 (6)	−0.0023 (5)
C7	0.0182 (7)	0.0179 (7)	0.0188 (6)	0.0029 (5)	−0.0006 (5)	−0.0013 (5)
C8	0.0209 (7)	0.0156 (7)	0.0211 (7)	0.0039 (5)	0.0000 (5)	−0.0026 (5)
C9	0.0193 (7)	0.0168 (7)	0.0196 (6)	0.0019 (5)	−0.0013 (5)	−0.0003 (5)
C10	0.0271 (8)	0.0153 (7)	0.0241 (7)	0.0006 (5)	−0.0006 (6)	−0.0016 (5)
C11	0.0293 (8)	0.0190 (7)	0.0249 (7)	−0.0038 (6)	0.0007 (6)	0.0018 (6)
C12	0.0228 (8)	0.0263 (8)	0.0238 (7)	−0.0020 (6)	0.0045 (6)	−0.0004 (6)
C13	0.0207 (7)	0.0198 (7)	0.0229 (7)	0.0005 (5)	0.0023 (5)	−0.0039 (5)
C14	0.0178 (7)	0.0172 (7)	0.0182 (6)	0.0008 (5)	−0.0003 (5)	−0.0017 (5)
C15	0.0197 (7)	0.0173 (7)	0.0220 (7)	0.0012 (5)	0.0033 (5)	−0.0005 (5)
C17	0.0243 (8)	0.0173 (7)	0.0269 (7)	0.0010 (6)	0.0047 (6)	−0.0062 (6)

Geometric parameters (Å, º)

O16—N16	1.2932 (15)	C8—H8	0.9500
N16—C15	1.2975 (18)	C8—C9	1.3924 (19)
N16—C17	1.4785 (16)	C9—C10	1.4324 (19)
C1—C2	1.4108 (19)	C9—C14	1.4381 (18)
C1—C14	1.4172 (18)	C10—H10	0.9500
C1—C15	1.4757 (18)	C10—C11	1.360 (2)
C2—C3	1.4332 (18)	C11—H11	0.9500
C2—C7	1.4396 (18)	C11—C12	1.4229 (19)
C3—H3	0.9500	C12—H12	0.9500
C3—C4	1.3631 (19)	C12—C13	1.3618 (19)
C4—H4	0.9500	C13—H13	0.9500
C4—C5	1.4217 (19)	C13—C14	1.4323 (19)
C5—H5	0.9500	C15—H15	0.9500
C5—C6	1.356 (2)	C17—H17A	0.9800
C6—H6	0.9500	C17—H17B	0.9800
C6—C7	1.4293 (19)	C17—H17C	0.9800
C7—C8	1.3968 (18)		
O16—N16—C15	125.30 (12)	C8—C9—C10	121.67 (12)
O16—N16—C17	114.96 (11)	C8—C9—C14	119.50 (12)
C15—N16—C17	119.73 (12)	C10—C9—C14	118.84 (12)
C2—C1—C14	120.37 (11)	C9—C10—H10	119.4
C2—C1—C15	122.40 (12)	C11—C10—C9	121.13 (13)
C14—C1—C15	117.05 (11)	C11—C10—H10	119.4
C1—C2—C3	122.93 (11)	C10—C11—H11	119.9
C1—C2—C7	119.48 (12)	C10—C11—C12	120.11 (13)
C3—C2—C7	117.57 (12)	C12—C11—H11	119.9
C2—C3—H3	119.4	C11—C12—H12	119.6
C4—C3—C2	121.17 (12)	C13—C12—C11	120.74 (13)
C4—C3—H3	119.4	C13—C12—H12	119.6
C3—C4—H4	119.6	C12—C13—H13	119.4

C3—C4—C5	120.90 (13)	C12—C13—C14	121.18 (13)
C5—C4—H4	119.6	C14—C13—H13	119.4
C4—C5—H5	120.0	C1—C14—C9	119.45 (12)
C6—C5—C4	119.91 (13)	C1—C14—C13	122.54 (12)
C6—C5—H5	120.0	C13—C14—C9	118.00 (12)
C5—C6—H6	119.4	N16—C15—C1	125.01 (13)
C5—C6—C7	121.29 (12)	N16—C15—H15	117.5
C7—C6—H6	119.4	C1—C15—H15	117.5
C6—C7—C2	119.07 (12)	N16—C17—H17A	109.5
C8—C7—C2	119.44 (12)	N16—C17—H17B	109.5
C8—C7—C6	121.49 (12)	N16—C17—H17C	109.5
C7—C8—H8	119.1	H17A—C17—H17B	109.5
C9—C8—C7	121.75 (12)	H17A—C17—H17C	109.5
C9—C8—H8	119.1	H17B—C17—H17C	109.5

O16—N16—C15—C1	0.9 (2)	C8—C9—C10—C11	−179.17 (13)
C1—C2—C3—C4	−178.89 (12)	C8—C9—C14—C1	0.08 (19)
C1—C2—C7—C6	178.96 (12)	C8—C9—C14—C13	179.06 (12)
C1—C2—C7—C8	−1.51 (19)	C9—C10—C11—C12	−0.4 (2)
C2—C1—C14—C9	−0.90 (19)	C10—C9—C14—C1	−179.40 (12)
C2—C1—C14—C13	−179.83 (12)	C10—C9—C14—C13	−0.42 (19)
C2—C1—C15—N16	56.39 (19)	C10—C11—C12—C13	0.6 (2)
C2—C3—C4—C5	−0.7 (2)	C11—C12—C13—C14	−0.7 (2)
C2—C7—C8—C9	0.7 (2)	C12—C13—C14—C1	179.59 (13)
C3—C2—C7—C6	−2.96 (19)	C12—C13—C14—C9	0.6 (2)
C3—C2—C7—C8	176.56 (12)	C14—C1—C2—C3	−176.36 (12)
C3—C4—C5—C6	−1.8 (2)	C14—C1—C2—C7	1.61 (19)
C4—C5—C6—C7	1.9 (2)	C14—C1—C15—N16	−128.50 (14)
C5—C6—C7—C2	0.5 (2)	C14—C9—C10—C11	0.3 (2)
C5—C6—C7—C8	−179.00 (13)	C15—C1—C2—C3	−1.4 (2)
C6—C7—C8—C9	−179.77 (12)	C15—C1—C2—C7	176.56 (12)
C7—C2—C3—C4	3.1 (2)	C15—C1—C14—C9	−176.11 (11)
C7—C8—C9—C10	179.46 (12)	C15—C1—C14—C13	4.96 (19)
C7—C8—C9—C14	0.0 (2)	C17—N16—C15—C1	179.78 (12)

Hydrogen-bond geometry (Å, º)

D—H···*A*	*D*—H	H···*A*	*D*···*A*	*D*—H···*A*
C15—H15···O16^{i}	0.95	2.24	3.1267 (18)	154
C17—H17*B*···O16^{i}	0.98	2.28	3.2037 (18)	157

Symmetry code: (i) *x*+1, *y*, *z*.